

A trinuclear Mo-Fe-Mo cluster compound $[\text{Et}_4\text{N}]\{[\text{Me}_2\text{dtcMoO}(\mu\text{-S})_2]_2\text{Fe}\}$ containing dialkyldithiocarbamate ligand

ZHANG, Yan-Shi(张琰澍) LIU, Qiu-Tian*(刘秋田) ZHU, Hong-Ping(朱红平)
CHEN, Yi-Hui(陈轶晖) CHEN, Chang-Neng(陈昌能)

State Key Laboratory of Structural Chemistry, Fujian Institute of Research on the Structure of Matter,
Chinese Academy of Sciences, Fuzhou, Fujian 350002, China

A trinuclear linear Mo-Fe-Mo dialkyldithiocarbamate complex $[\text{Et}_4\text{N}]\{[\text{Me}_2\text{dtcMoO}(\mu\text{-S})_2]_2\text{Fe}\}$ has been obtained and structurally characterized, which contains two $\text{Me}_2\text{dtcMoO}(\mu\text{-S})_2$ units coordinated to a central tetrahedral Fe atom. A comparison of the structural parameters indicates the metal oxidation states of $2\text{Mo}(\text{V}) + \text{Fe}(\text{III})$. The ^1H NMR shows chemical shifts of Me_2dtc ligands at δ 10.14 and δ 9.40 with the intensity ratio of 1:1. The cyclic voltammogram displays a reversible couple at $-1.41\text{ V}/-1.36\text{ V}$ responsible for 1-/2-anions of the complex and an irreversible oxidation at 0.5 V , which seems to show the apparent lack of stability for its neutral species $(\text{Me}_2\text{dtcMoOS}_2)_2\text{Fe}$.

Keywords Iron complex, molybdenum complex, dialkyldithiocarbamate, crystal structure, spectrum, electrochemistry

Introduction

Over the last two decades, the inorganic modeling of the structure and function of active centers of metallo-proteins has been of an increased interest. Much effort has been focused on the Mo/Fe/S cluster contained in FeMo-cofactor of nitrogenase. Trinuclear Mo-Fe-Mo cluster $[(\text{MoS}_4)_2\text{Fe}]^{3-}$ with $\text{Mo}(\mu\text{-S})_2\text{Fe}$ structural units was one of the early modeling compounds and was intensively studied¹ in order to mimic the spectral properties of this natural active center. Up to now, a trinuclear linear Mo/Fe/S cluster family has appeared to contain Mo-Fe-Mo,^{1,2} Fe-Mo-Fe,³ and Fe-Fe-Mo⁴ complexes, of which $\text{Mo}(\mu\text{-S})_2\text{Fe}(\mu\text{-S})_2\text{Mo}$ complexes have become an important type. However, none of these lin-

ear complexes contains dialkyldithiocarbamate (R_2dtc) ligand though a tetranuclear Mo-Fe-Fe-Mo cluster⁵ and a series of Mo/Fe/S cubane-like clusters⁶ have been reported to contain R_2dtc ligands. This paper reports a novel member of trinuclear Mo-Fe-Mo cluster family, which is the first trinuclear linear Mo-Fe-S cluster containing R_2dtc ligand.

Experimental

All manipulations were carried out under dinitrogen atmosphere. The solvents were dried with molecular sieves and degassed prior to use. Ferrous chloride and Et_4NCl are commercially available without further purification. Compound $(\text{NH}_4)_2\text{MoO}_2\text{S}_2$ was obtained by literature method.⁷ Me_2dtcNa was synthesized by the reaction of Me_2NH with NaOH and CS_2 in water.

Preparation of $[\text{Et}_4\text{N}]\{[\text{Me}_2\text{dtcMoO}(\mu\text{-S})_2]_2\text{Fe}\}$ (1)

A solution of FeCl_2 (0.76 g, 6 mmol), Me_2dtcNa (1.71 g, 12 mmol) and Et_4NCl (0.33 g, 2 mmol) in 16 mL of DMF was stirred vigorously for one hour, then $(\text{NH}_4)_2\text{MoO}_2\text{S}_2$ (0.46 g, 2 mmol) was added. The solution was stirred for 34 h. After filtration, 12 mL of MeCN was added to the filtrate, and the solution was allowed to stand at 4°C for two days. After filtration to remove precipitates, 10 mL of acetonitrile was added to the solution and the solution was allowed to stand for several days. Black crystals were collected, washed with ace-

Received June 29, 1999; accepted October 15, 1999.

Project (Nos. 29671031 and 29733090) supported by the National Natural Science Foundation of China.

tonitrile, and dried *in vacuo*, affording 0.34 g (yield 43.7%) of product. ν_{\max} (KBr): 1538(C-N, dtc), 933 (Mo = O), 436 (Mo- μ_2 S), 322, 375 (Mo-Sdtc) cm^{-1} . δ_{H} (DMSO- d_6): 1.16 (CH₃, Et₄N), 3.14 (CH₂, Et₄N), 9.40, 10.14 (CH₃, Me₂dtc). Anal. C₁₄H₃₂FeMo₂N₃O₂S₈. Calcd: C, 21.56; H, 4.11; Fe, 7.19; Mo, 24.65; N, 5.39. Found: C, 21.24; H, 3.99; Fe, 6.88; Mo, 24.04; N, 5.15.

Crystal structure determination

A black prism crystal of the title complex with approximate dimensions of 0.60 × 0.35 × 0.30 mm was coated with epoxy resin and mounted on a glass fibre. Data collection was performed with Mo K_{α} radiation ($\lambda = 0.071073$ nm) on an Enraf Nonium CAD₄ diffractometer at 20°C using ω -2 θ scan mode with the maximum 2 θ of 50°. A total of 5946 reflections were collected and the corrections of Lorentz polarization and empirical absorption were applied to the data. Summary of the crystal data, data collection and structure refinement of (Et₄N)-[(Me₂dtcMoOS₂)₂Fe] is listed in Table 1.

Table 1 Summary of crystal data, data collection and structure refinement of (Et₄N)-[(Me₂dtcMoOS₂)₂Fe]

Formula	C ₂₀ H ₄₆ FeMo ₂ N ₄ O ₂ S ₈
Mr	878.85
Color and habit	black prism
Crystal size/mm	0.60 × 0.35 × 0.30
System	monoclinic
Space group	C2/c
a/nm	1.8382(7)
b/nm	1.9782(7)
c/nm	2.0296(8)
$\beta/^{\circ}$	116.87(3)
Z	8
$D_c/\text{g}\cdot\text{cm}^{-3}$	1.77
μ/cm^{-1}	16.8
$F(000)$	3128
Total reflections	5946
Observed reflections	1808 ($I > 3.0\sigma(I)$)
R^a	0.0888
R_w^b	0.0929
No. of variables	266
S (goodness of fit)	1.00
Residual peak/ $\text{e}\cdot\text{nm}^{-3}$	500 to -170

$$^a R = \sum |F_o - F_c| / \sum |F_o|$$

$$^b R_w = [(\sum w(F_o - F_c)^2 / \sum w F_o^2)]^{1/2}$$

The structure of complex **1** was solved by direct methods with MULTAN-83 program followed by successive difference Fourier syntheses. The structure was refined in full-matrix least-squares method using anisotropic thermal parameters for all the non-hydrogen atoms. All hydrogen atoms were geometrically located and included in the structure factor calculations, but their positions were not refined. The final cycle of refinement included 266 variable parameters for 1536 reflections with $I > 3.0\sigma(I)$ and converged to $R = 0.089$ and $R_w = 0.093$. The highest peak in the final difference Fourier map had a maximum height of 500 e/nm^3 , and the minimum negative peak of -170 e/nm^3 . All calculations were performed on a COMPAQ computer using MolEN/PC program.⁸

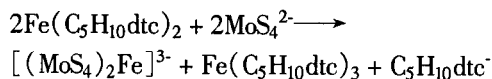
Other physical measurement

Infrared spectrum was recorded on a Bio-Rad FTS-40 model spectrophotometer. ¹H NMR spectrum was recorded on a Bruker-Am 500 spectrometer with TMS as standard. Electrochemical measurement was performed in cyclic voltammetric mode on a CV-1B cyclic voltammeter in DMF solution with an SCE reference electrode, Pt plate working electrode and Pt auxiliary electrode. The supporting electrolyte was Et₄NBF₄.

Result and discussion

Synthesis

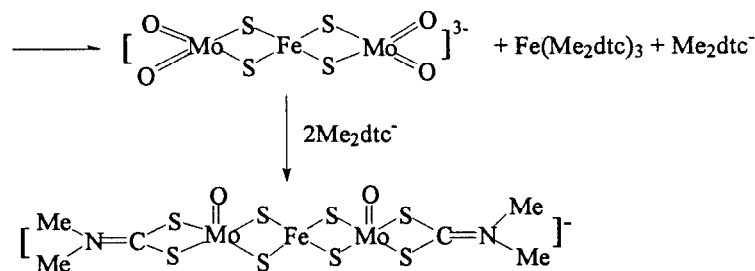
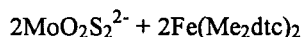
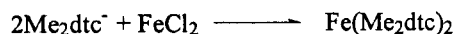
Complex **1** was obtained from an assembly system composed of MoO₂S₂²⁻, FeCl₂, Me₂dtc⁻ and Et₄N⁺. The formation of **1** passes through coordination of MoO₂S₂²⁻ and redox of the metal centers. In the reaction MoO₂S₂²⁻ acts as a bidentate ligand chelating to the Fe center, accompanying with the reduction of MoO₂S₂²⁻. A series of reactions of MoS₄²⁻ and Fe²⁺ with reducing agents (R₂dtc⁻, ROCSS⁻, PhS⁻ etc.) have resulted in the trinuclear cluster [(MoS₄)₂Fe]³⁻,¹ such as the following reaction reported by Newton.^{1b}



It is believed that a similar trianion [(MoO₂S₂)₂-

$\text{Fe}]^{3-}$ would become a possible intermediate in our reaction system and then undergoes a replacement of Me_2dtc

group leading to the production of the title complex as shown in the following mechanism:



Though the $\text{Mo}=\text{O}$ bonding is strong in $\text{Mo}^{(\text{V})}$ complex, the example in which the terminal oxygen atom is substituted by nucleophilic sulfur ligand has been reported and discussed.⁹

Structure

The structure of compound **1** is composed of a monoanion shown in Fig. 1 and one $[\text{Et}_4\text{N}]^+$ cation. Selected bond distances and angles are listed in Table 2. A tetrahedrally coordinated Fe atom is bounded to two $[(\text{Me}_2\text{dtc})\text{MoOS}_2]^{2-}$ units through two bridging sulfido-groups, forming a nearly linear trinuclear backbone with the Fe-Mo-Fe bond angle of 168.6° . The Fe-S bond distances range from $0.2183(6)$ to $0.2233(8)$ nm with the mean value of $0.2217(10)$ nm, which is consistent with the $\text{Fe}^{(\text{III})}-\text{S}$ distances in compounds $[\text{Me}_4\text{N}]_3\{[(\text{SCH}_2\text{CH}_2\text{S})\text{MoS}_3]_2\text{Fe}\}$ ($0.2221(6)$ nm)^{2a} and $[\text{Et}_4\text{N}]_3\{[(\text{SCH}_2\text{CH}_2\text{S})\text{MoS}_3]_2\text{Fe}\}$ (0.2225 nm)^{2b}

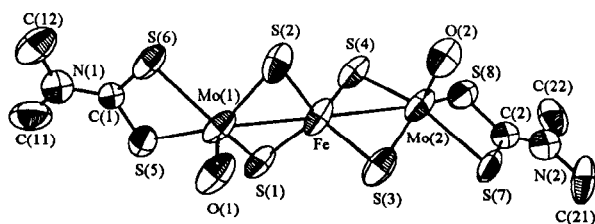


Fig. 1 Structure and labeling of $[(\text{Me}_2\text{dtcMoO}(\mu\text{-S})_2)_2\text{Fe}]^{3-}$. Thermal ellipsoids as drawn by ORTEP represent the 30% probability surfaces.

Table 2 Selected bond distances (nm) and angles ($^\circ$)

Distance			
Mo(1)—Fe	0.2697(4)	Mo(2)—Fe	0.2691(4)
Mo(1)—S(1)	0.2316(6)	Mo(2)—S(3)	0.2305(7)
Mo(1)—S(2)	0.2299(9)	Mo(2)—S(4)	0.2297(9)
Mo(1)—S(5)	0.246(1)	Mo(2)—S(7)	0.2449(7)
Mo(1)—S(6)	0.2472(7)	Mo(2)—S(8)	0.2442(7)
Mo(1)—O(1)	0.170(2)	Mo(2)—O(2)	0.165(2)
Fe—S(1)	0.2232(9)	Fe—S(2)	0.2233(8)
Fe—S(3)	0.222(1)	C(1)—N(1)	0.144(3)
Fe—S(4)	0.2183(6)	C(2)—N(2)	0.126(3)
Angle			
Mo(1)—Fe—Mo(2)	168.6(2)		
S(1)—Mo(1)—S(2)	102.8(3)	S(5)—Mo(1)—S(6)	70.3(3)
S(1)—Mo(1)—S(6)	140.4(3)	S(1)—Mo(1)—S(5)	81.1(3)
S(2)—Mo(1)—S(6)	85.0(3)	S(2)—Mo(1)—S(5)	141.9(3)
S(1)—Mo(1)—O(1)	108.5(6)	S(2)—Mo(1)—O(1)	107.2(8)
S(5)—Mo(1)—O(1)	107.2(8)	S(6)—Mo(1)—O(1)	105.9(6)
S(3)—Mo(2)—S(4)	101.7(3)	S(7)—Mo(2)—S(8)	69.9(2)
S(3)—Mo(2)—S(7)	85.1(2)	S(3)—Mo(2)—S(8)	141.6(3)
S(4)—Mo(2)—S(7)	140.5(3)	S(4)—Mo(2)—S(8)	82.2(3)
S(3)—Mo(2)—O(2)	106.6(5)	S(4)—Mo(2)—O(2)	109.5(7)
S(7)—Mo(2)—O(2)	105.4(7)	S(8)—Mo(2)—O(2)	107.9(5)
S(1)—Fe—S(2)	107.8(3)	S(1)—Fe—S(3)	110.2(3)
S(1)—Fe—S(4)	106.1(3)	S(2)—Fe—S(3)	114.8(3)
S(2)—Fe—S(4)	109.5(3)	S(3)—Fe—S(4)	108.2(3)

indicating that the Fe oxidation state in **1** is the same as those of the complexes containing a tetrahedral FeS_4 unit. Both the five-coordinate Mo sites possess distorted tetragonal pyramid coordination geometry with $\text{S}(1)-$

S(2)-S(5)-S(6) and S(3)-S(4)-S(7)-S(8) based planes for Mo(1) and Mo(2), respectively. The Mo—S bond distances can be divided into two sets one of which is Mo—S_{core} (0.2297(9)—0.2316(6) nm) and the other Mo—S_{dtc} (0.2442(7)—0.2472(7) nm). The Mo coordination geometry is identical to that found in the binuclear Mo^(V) complexes, Mo₂O₂(μ-S)₂(dtc)₂¹⁰ and Mo₂O₂(μ-S)₂(C₄H₈dtc)₂,¹¹ and the corresponding bond lengths are similar to each other in these complexes (Table 3), indicating that Mo⁵⁺ and Fe³⁺ are reasonable oxidation states for **1**. Electron transfer from Fe^(II) to Mo^(VI) through the double sulfido bridges gives rise to

the reduction of MoO₂S₂²⁻ moiety with the formation of the complex and explains the variation of metal oxidation state. The mean Mo—Fe bond length is 0.2695 nm, showing significant metal-metal interaction between Mo and Fe atoms. Interestingly, distinguishable structural features were observed between the two Mo atoms. For example, Mo(1)—S_{dtc} and Mo(1)—O bond distances are longer than Mo(2)—S_{dtc} and Mo(2)—O by 0.002 nm and 0.005 nm, respectively, and C(1)—N(1) (0.144(3) nm) is obviously longer than C(2)—N(2) (0.126(3) nm). This may lead to some differences in the spectral features for the two Mo atoms.

Table 3 Comparison of bond distances (nm) and angles (°) for related Mo/Fe/S complexes

Compound	Mo—S _{core}	Mo—S _{dtc}	Fe—S _{core}	Mo = O	Mo-Fe-Mo	Ref.
[(Me ₂ dtcMoOS ₂) ₂ Fe] ³⁻	0.2304(8)	0.246(1)	0.2217(10)	0.168(2)	168.6(2)	<i>a</i>
{[(C ₂ H ₄ S ₂)MoS ₃] ₂ Fe} ³⁻	0.232(1)		0.2221(6)		155.7(2)	[2a]
{[Mo ₂ O ₂ S ₂ (S ₂) ₂ Fe] ³⁻	0.231(1)		0.225(1)	0.168(2)	160.3(2)	[2b]
Mo ₂ O ₂ S ₂ (dtc) ₂	0.2325(1)	0.2461(1)		0.1677(3)		[10]
Mo ₂ O ₂ S ₂ (C ₄ H ₈ dtc) ₂	0.2318(3)	0.2464(2)		0.1660(5)		[11]

^a This work.

Infrared spectra

The R₂dtc ligands have very characteristic absorption in the vicinity of 1500 cm⁻¹ corresponding to the stretching vibration of C—N.¹² The C—N stretching vibration of compound **1** was observed at 1538 cm⁻¹ showing considerable double-bond character. This is consistent with the short C—N bond distance (< 0.140 nm) in the compound. The vibrations of Mo = O and Mo—μ₂S occur at 933 cm⁻¹ and 436 cm⁻¹, respectively. The absorptions at 322 cm⁻¹ and 375 cm⁻¹ are attributed to the Mo—S_{dtc} vibration.¹²

¹H NMR spectrum

The ¹H NMR spectrum of **1** in DMSO-*d*₆ is depicted in Fig. 2. It is noticed that Me₂dtc ligand coordinating to the metal atom forms a MS₂C = NMe₂ conjugation system through which the paramagnetic metal site affects the proton chemical shift of the Me₂dtc group by the contact mechanism. This has been observed in some Mo⁶ and V¹³ complexes, which contain paramagnetic metal center linking to Me₂dtc group. In the spectrum of **1**, two peaks at δ 10.14 and δ 9.40 with the intensity

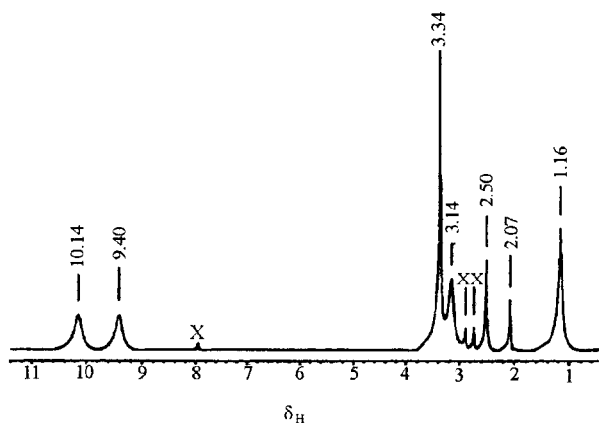


Fig. 2 ¹H NMR spectrum of [Et₄N][Me₂dtcMoO(μ-S)₂]₂Fe in DMSO-*d*₆ solution at room temperature. δ_H: 1.16(CH₃, Et₄N), 2.07(CH₃CN), 2.50(DMSO), 3.14(CH₂, Et₄N), 3.34(H₂O), 9.40, 10.14(Me₂dtc). The mark X represents DMF (HCO, 7.98; CH₃, 2.73, 2.89).

ratio of 1:1 can be assigned to the Me₂dtc groups that coordinate to the Mo^(V) sites, showing obviously down-field shift relative to the corresponding signal of Me₂dtcNa (δ 3.5, DMSO-*d*₆). The two peaks with i-

dential intensity imply that there are two types of distinguishable CH_3 groups in the complex. This can be considered to stem from either the two Mo sites having aforementioned significantly different structural parameters or the $\text{C}=\text{N}$ double bond restricting free rotation around the bond and making the two CH_3 groups of the same Mo site different from each other in ^1H NMR spectrum. However, the latter seems unlikely since the environments of the two methyl groups are almost identical. Therefore, it is reasonable to assign the two peaks as the contribution of Me_2dtc^- groups of Mo(1) and Mo(2), respectively.

Electrochemical study

The cyclic voltammogram diagram of **1** in DMF displays irreversible oxidation at 0.5 V and a reversible redox process at $-1.41\text{ V}/-1.36\text{ V}$ as shown in Fig. 3. Interestingly, this electrochemical behavior has somewhat similarity to that of $[(\text{MoS}_4)_2\text{Fe}]^{3-1a,b}$ which shows its irreversible oxidation at -0.10 V and quasireversible redox at $-1.798\text{ V}/-1.688\text{ V}$ in CH_3CN . Similarly,

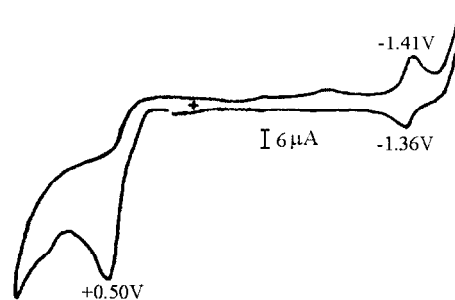


Fig. 3 Cyclic voltammogram for complex **1**, 0.002 mol/L in DMF with scan speed of 100 mV/s.

we tentatively assign the latter couple ($-1.41\text{ V}/-1.36\text{ V}$) to the reduction of $[(\text{Me}_2\text{dtcMoOS}_2)_2\text{Fe}]^-$. It is shown that the $\text{Mo}(\mu\text{-S})_2\text{Fe}(\mu\text{-S})_2\text{Mo}$ backbone has its ability to delocalize charge by accepting electron in unoccupied Mo-d orbitals. Such reductions have also been reported for $[\text{M}'-(\text{MS}_4)_2]^{2-}$ complexes¹⁴ ($\text{M}' = \text{Ni}, \text{Pd}, \text{Pt}, \text{Co}$; $\text{M} = \text{Mo}, \text{W}$). However, the irreversibility of the oxidation at 0.5 V seems to show the apparent lack of stability for its neutral species $(\text{Me}_2\text{dtcMoOS}_2)_2\text{Fe}$.



References

1. a) Coucouvanis, D.; Simhon, E. D.; Beenziger, N. C., *J. Am. Chem. Soc.*, **102**, 6646(1980).
b) Friesen, G. D.; McDonald, J. W.; Newton, W. E.; Euler, W. B.; Hoffman, B. M., *Inorg. Chem.*, **22**, 2202(1983).
c) Liu, H. Q.; Liu, Q. T.; Kang, B. S.; He, L. J.; Chen, C. N.; Zhao, K.; Hong, M. C.; Huang, L. R.; Zhuang J.; Lu, J. X., *Scientia Sinica*, **B31**, 10 (1988).
2. a) Dahlstrom, P. L.; Kumar, S.; Zubieta, J., *J. Chem. Soc., Chem. Commun.*, 411(1981).
b) Zhang, Z. Z.; Wang, F. S.; Fan, Y. G., *Kexue Tongbao* (in Chinese), **29**, 1486(1984).
c) Xu, L. J.; Wang, F. S.; Lu, P. J.; Fan, Y. G., *Scientia Sinica*, **B27**, 877(1984).
d) Xu, J. Q.; Liu, X. S.; Li, S. Q.; Fan, Y. G.; Wang, F. S.; Lu, P. J., *Kexue Tongbao*, **29**, 344 (1984).
3. Coucouvanis, D.; Baenziger, N. D.; Simhon, E. D.; Strempel, P.; Swenson, D.; Simpopoulos, A.; Kostikas, A.; Petrouleas, V.; Papaefthymios, V., *J. Am. Chem. Soc.*, **102**, 1732(1980).
4. Tieckelmann, R. H.; Averill, B. A., *Inorg. Chim. Acta*, **46**, L35(1980).
5. Liu, Q. T.; Huang, L. R., *Jiegou Huaxue* (Chinese J. Struct. Chem.), **10**, 10(1991).
6. Liu, Q. T.; Huang, L. R.; Liu, H. Q.; Lei, X. J.; Wu, D. X.; Kang, B. S.; Lu, J. X., *Inorg. Chem.*, **29**, 4131(1990).
7. McDonald, J. W.; Friesen, G. D.; Rosenheim, L. D.; Newton, W. E., *Inorg. Chim. Acta*, **72**, 205(1983).
8. *MolEN, An Interactive Structure Solution Procedure*, Enraf-Nonius, Delft, The Netherlands, 1990.
9. Hu, Y. H.; Weng, L. H.; Kang, B. S., *Jiegou Huaxue* (Chinese J. Struct. Chem.), **10**, 84(1991).
10. Howlader, N. C.; Haight, G. P.; Hambley Jr., T. W.; Snow, M. R.; Lawrance, G. A., *Inorg. Chem.*, **23**, 1811(1984).

-
11. Lu, S.F.; Huang, J.Q.; Chen H.B.; Wu, Q.J., *Acta Chim. Sin.* (in Chinese), **51**, 885(1993).
12. Bradley D.C.; Gitlitz, M.H., *J. Chem. Soc., A*, 1152(1969).
13. a) Yang, Y.; Liu Q.T.; Wu, D.X., *Inorg. Chim. Acta*, **208**, 85(1993).
b) Zhu, H.P.; Liu, Q.T.; Deng, Y.H.; Wen, T.B.; Chen C.N.; Wu, D.X., *Inorg. Chim. Acta*, **268**, 7 (1999).
14. a) Callahan K.P.; Piliero, P.A., *J. Chem. Soc., Chem. Commun.*, **19**, 13(1979).
b) Callahan K.P.; Piliero, P.A., *Inorg. Chem.*, **19**, 2619(1980).
c) Müller, A.; Jostes, R.; Flemming V.; Potthest, R., *Inorg. Chim. Acta*, **44**, L33(1980).

(E9906073 SONG, J.P.; LING, J.)